Chemical Engineering and Processing 55 (2012) 8–19

Contents lists available at SciVerse ScienceDirect

Chemical Engineering and Processing: Process Intensification

journal homepage: www.elsevier.com/locate/cep

# Hydrodynamic features of centrifugal contactor separators: Experimental studies on liquid hold-up, residence time distribution, phase behavior and drop size distributions

Boelo Schuur[a,b,*], Gerard N. Kraai[a,1], Jozef G.M. Winkelman[a,1], Hero J. Heeres[a,1]

[a] University of Groningen, Department of Chemical Engineering, Nijenborgh 4, 9747 AG, Groningen, The Netherlands
[b] University of Twente, Faculty of Science and Technology, Thermo-Chemical Conversion of Biomass group. P.O. Box 217, 7500 AE, Enschede, The Netherlands

ARTICLE INFO

*Article history:*
Received 28 November 2011
Received in revised form 20 February 2012
Accepted 22 February 2012
Available online 2 March 2012

*Keywords:*
Process intensification
Centrifugal contactor separator
Hydrodynamics
Residence time distribution
Phase inversion
Drop size distribution

ABSTRACT

The liquid hold-up, residence time distributions (RTD), drop size distributions and continuous/dispersed phase for a typical centrifugal contactor separator (CCS) of the type CINC V02 were determined experimentally for various L-L systems. The hold-up ratio of the different solvents was mainly a function of the selected weir. Most of the liquids reside in the centrifuge, whereas the annular zone is only partly filled as was determined for four water–organic (heptane, toluene, 1-octanol and dichloroethane) systems. The macro-mixing pattern of both liquid phases was determined experimentally using step responses for several aqueous–organic solvent combinations. Fitting the experimental curves to a standard tanks-in-series model without dead zone yielded large errors, very good fits were obtained for typically seven (continuous phase) or more (dispersed phase) tanks in series with a dead zone of typically about 20 mL. Drop size distribution measurements using a FBRM probe for various solvent combinations showed that the Sauter mean drop sizes of the dispersed phase were between 30 and 600 μ. The small drops indicate a very high specific interfacial area in the annular zone of up to 10 times the specific interfacial area in stirred tanks. Phase inversion was observed for several solvent combinations (e.g. water–1-octanol, water–dichloromethane and water–dichloroethane) and was found to be perfectly reversible.


## 1. Introduction

Process intensification (PI) is a powerful concept to replace large, energy intensive equipment or processes with smaller plants that combine multiple operations in single, highly integrated devices [1]. Well-known separations integrated with reactions in a single device are reactive-distillation [2], chromatography, adsorption and extraction [3,4]. For the latter, the integration of reaction and separation is advantageous not only with respect to energy and investment costs but also for efficiency and/or the selectivity improvement of the extraction process [5–7].

A very attractive device to integrate chemical reaction and separation for liquid–liquid systems is a centrifugal contactor separator (CCS). The CCS has been developed at the Argonne National Laboratory in the USA. An improved version was patented under the trade name CINC by Costner Industries Nevada Corporation [8]. The CINC basically consists of a rotating hollow centrifuge in a static house. The liquids enter the device in the annular zone between the static wall and the rotating centrifuge, where they are intensely mixed. Subsequently, they are transferred into the centrifuge through a hole in the bottom where separation occurs by the action of centrifugal forces. A low-mix configuration may be used to avoid direct contact of the entering liquids with the centrifuge. Also, one of the liquids can be introduced directly into the centrifuge through the bottom plate of the device. These different configurations are depicted in Fig. 1. Characteristic features of the CINC V02 are tabulated in Table 1.

The CCS was initially developed for clean-up of nuclear waste [9]. Other applications like oil–water separations and liquid–liquid extractions were claimed in a patent issued by Meikrantz [8]. Open source literature in which the CCS is used for combined chemical reaction and integrated separation is scarce and only devoted to reactive extractions [10–13]. With the recent attention for process intensification and integration [1,2,4], we have performed studies aiming at the use of the CCS for continuous biphasic (bio)catalysis [14] and enantioselective liquid–liquid extraction [15–18].

* Corresponding author at: University of Twente, Faculty of Science and Technology, Thermo-Chemical Conversion of Biomass group. P.O. Box 217, 7500 AE, Enschede, The Netherlands. Tel.: +31 53 489 2891;
fax: +31 53 489 4738/50 363 4479.
*E-mail addresses:* b.schuur@utwente.nl (B. Schuur), gerard@kraai.biz (G.N. Kraai), j.g.m.winkelman@rug.nl (J.G.M. Winkelman), h.j.heeres@rug.nl (H.J. Heeres).
[1] Fax: +31 50 363 4479.

0255-2701/$ – see front matter © 2012 Elsevier B.V. All rights reserved.
doi:10.1016/j.cep.2012.02.008

**Nomenclature**

| | |
|---|---|
| $a$ | specific interfacial area per volume dispersion [$m^2/m^3$ liquid] |
| AQBF | configuration of the CINC V02 where the aqueous phase enters directly in the centrifuge through the bottom |
| C | Cinchona alkaloid, extractant in DCE |
| $d$ | diameter [m] |
| $\overline{d_{vs}}$ | Sauter mean drop size [m] |
| DCE | 1,2-dichloroethane |
| DCM | dichloromethane |
| DNB-leu | 3,5-dinitrobenzoyl-*(R)*,*(S)*-Leucine, used as aqueous solution for drop size distribution measurements |
| Exp | experiment |
| $f$ | relative frequency [−] |
| $F$ | cumulative residence time distribution function [−] |
| $F$ | flow rate [mL/min] |
| HM | high mix, a configuration of the CINC V02 |
| $h$ | heavy phase |
| $l$ | light phase |
| LM | low mix, a configuration of the CINC V02 |
| $n$ | index for tank number in tanks-in-series model [−] |
| $N$ | number of tanks in series [−] |
| ORGBF | configuration of the CINC V02 where the aqueous phase enters directly in the centrifuge through the bottom |
| $t$ | time [min] |
| $V$ | Volume (hold-up) [mL] |

*Greek letters*

| | |
|---|---|
| $\varepsilon$ | hold-up fraction [−] |
| $\upsilon$ | rotational frequency [Hz] |
| $\phi_v$ | volumetric flow rate [mL/min] |
| $\tau$ | average residence time [min] |
| $\Omega$ | resistance [Ω] |
| $\rho$ | density [$kg/m^3$] |
| $\sigma$ | interfacial tension [$mN/m = 10^{-3}\ kg/s^2$] |

*Subscripts*

| | |
|---|---|
| ANN | annular zone |
| CENTR | centrifuge |
| aq | aqueous phase |
| d | dead zone |
| i | index for drop size classes |
| k | index for phase (k = aq, org) |
| n | index for mixer in mixers in series model |
| org | organic phase |
| tot | total |

For reactor modeling purposes, detailed information is required on hydrodynamic properties of the CCS such as the liquid hold-ups, (specific) interfacial areas, macro-mixing pattern and phase behavior. Although the use of CCS equipment has been reported extensively [19], only a few studies on the hydrodynamics of CCS equipment have been published. Schuur et al. determined the interfacial area in the CINC experimentally for a biphasic system containing aqueous hydroxide solution and *n*-butyl formate as the organic phase [20], recently Wardle et al. studied the effect of vane geometries on operation characteristics [21,22], and a number of computational fluid dynamics (CFD) studies were reported [23–27]. Here we present the results of hydrodynamic studies in a typical CCS device, the CINC V02. This table-top device has a geometric volume of 322 mL and may be operated at a maximum throughput of 1.9 L/min.

## 2. Theory

### 2.1. Residence time distribution curves

Residence time distribution (RTD) curves give valuable information on the overall flow pattern of the liquid phases in the CCS. The CCS may be spatially separated into three distinct zones. The liquids enter the device in the annular zone, where intense mixing occurs. In the centrifuge, both phases are settled. Subsequently, the liquids pass through a set of collector ring channels in the upper part of the device. The overall RTD of the CCS will be determined by the flow pattern in each of these zones.

Experimentally, the response of the CCS device to a step function in the feed was measured at both the entrance and the exit of the CCS. These concentration profiles were normalized to obtain an *F*-curve (Eq. 1):

$$F(t) = \frac{C(t)}{C_{step}}. \tag{1}$$

The experimental RTD curves of the CCS were obtained by correction of the outlet signal with the inlet signal, and compared with the standard tanks tanks-in-series model and a modified model including a dead zone volume. A schematic representation of the model with the dead zone is given in Fig. 2.

### 2.2. Drop size distributions in L-L systems

A key parameter for the modeling of L-L reactors is the specific interfacial area, defined as [28]:

$$a = \frac{6\varepsilon}{\overline{d_{vs}}}. \tag{2}$$

Here, $\varepsilon$ is the fraction of the dispersed phase and $\overline{d_{vs}}$ is the Sauter mean drop size, defined as [29]:

$$\overline{d_{vs}} = \frac{\sum_1^N n_i d_i^3}{\sum_1^N n_i d_i^2}. \tag{3}$$

In well-mixed systems, from the drop size distribution the specific interfacial area can be calculated using Eq. (2), assuming that the hold-up fraction of the dispersed phase equals the feed rate fraction [30].

### 2.3. Phase behavior in L-L systems

Experimental data on the continuous and dispersed phase and the occurrence of phase inversions as a function of process conditions and the physical properties of both liquids are not available for CCS devices. For stirred tank reactors, the phase with the highest hold-up is usually the continuous phase [31,32]. The organic phase hold-up ($\varepsilon = V_{org}/V_{tot}$) at which phase inversion occurs is a function of the physical properties of the fluids and the power input. Usually an ambivalent region exists where both phases may be continuous [31,32]. This region is usually caused by variations in the startup procedure [33]. Liu et al. recently demonstrated that the ambivalence region becomes smaller when increasing the power input. At high stirring speeds ambivalence may even be absent [34].

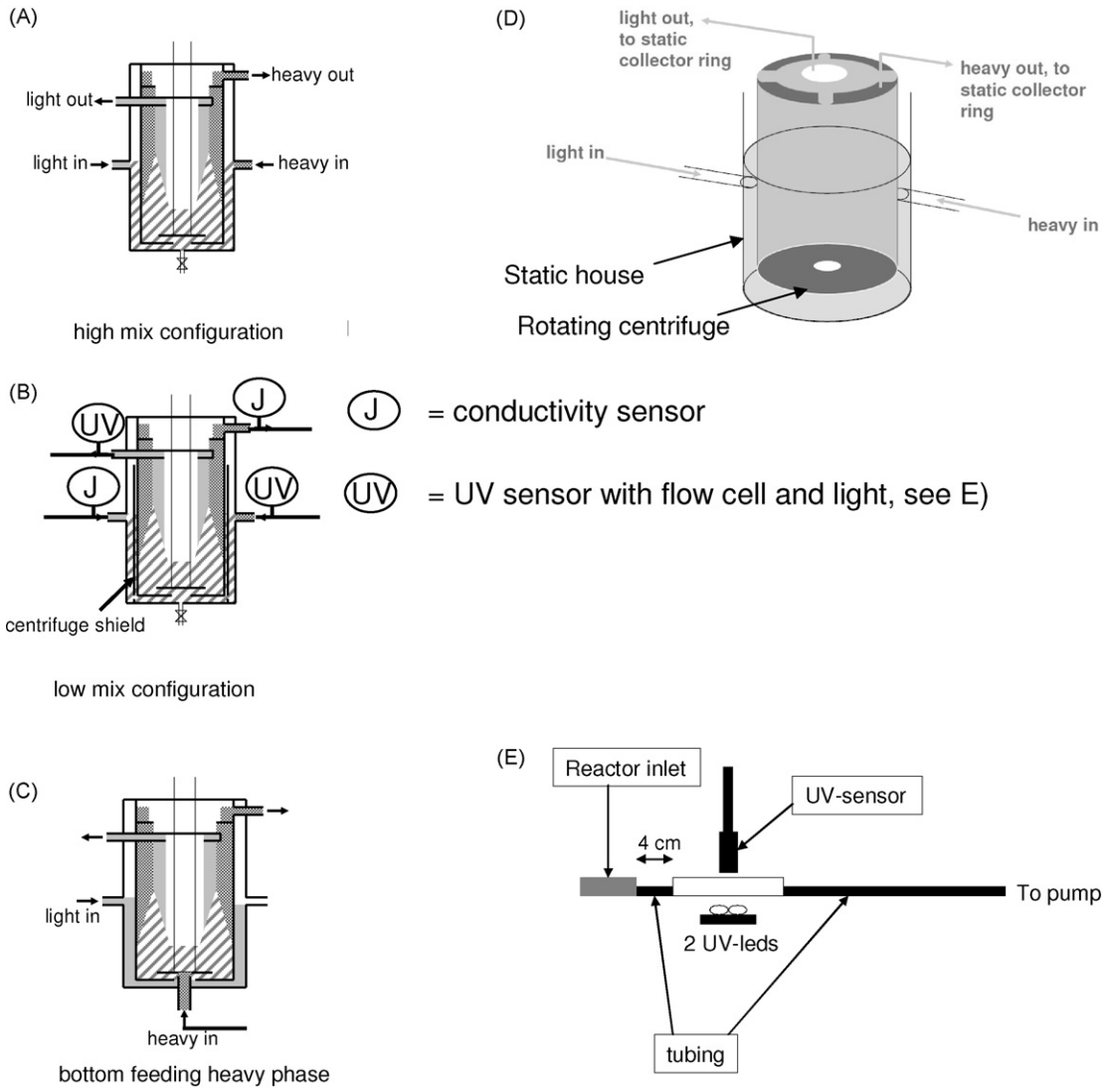


**Fig. 1.** Sketch of the CCS device showing different operational modes. (A) high mix; (B) low-mix (shielded centrifuge) equipped with sensors for RTD; (C) heavy phase fed directly in centrifuge through the bottom plate. For (A)–(C): Hatched: dispersion. Darker gray: heavy phase. Lighter gray: light phase; (D) scheme detailing the rotation of the centrifuge and the weir system; (E) detail of the UV-sensor setup.

**Table 1**
Geometry and properties of the CINC V02.

| Feature | Value | Dimensions | Comment |
|---|---|---|---|
| General features | | | |
| Maximum throughput | 1.9 | L/min | Total throughput for both phases |
| Rotor frequency | 0–100 | Hz | |
| Typical power consumption | 60 | W | We measured the power consumption from the grid, under typical operating conditions of 30–60 Hz, and low viscous fluids. Under these conditions the power consumption is rather constant at 60 W. Above 75 Hz, or when using highly viscous fluids, the power consumption strongly increases up to 130 W. |
| Geometry | | | |
| Diameter of house | 62 | mm | |
| Height annular zone from inlets to bottom | 70 | mm | |
| Spacing between bottom plate and centrifuge | 7 | mm | |
| Height vanes bottom plate | 5 | mm | |
| Outer diameter centrifuge | 50.75 | mm | |
| Inner diameter centrifuge | 50 | mm | |
| Height centrifuge from bottom to light phase weir | 99 | mm | |
| Light phase weir diameter | 20.64 | mm | The light phase weir is fixed, whereas the heavy phase weir is replaceable. |
| Heavy phase weir diameter | Variable | mm | The heavy phase weir size depends on the density difference of the liquids used. A Microsoft Excel macro is provided by the vendor to select the right weir. |

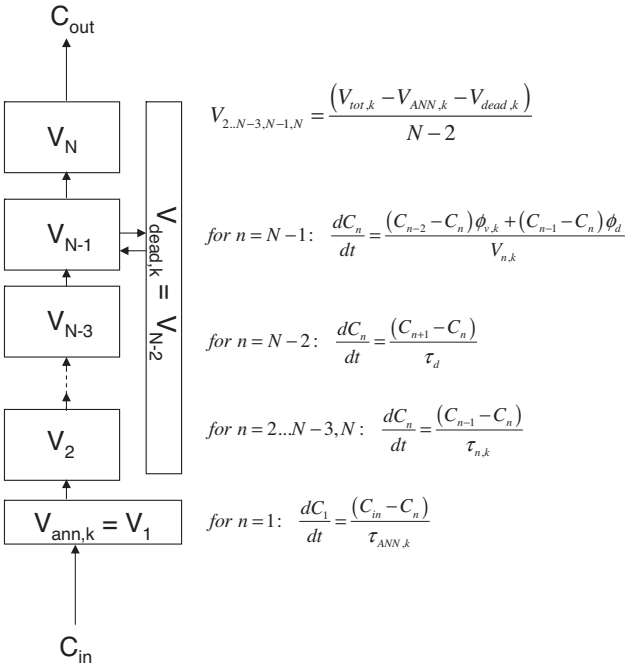


**Fig. 2.** Schematic representation of the mixers in series model with a dead-zone volume exchanging with mixer $N-1$.

## 3. Experimental

### 3.1. Chemicals

Reverse osmosis water was applied for all experiments. 1,2-Dichloroethane (99%), and 1-octanol (98%) were obtained from Sigma–Aldrich, potassium dihydrogen phosphate (*pa*) and di-sodium hydrogen phosphate dodecahydrate (*pa*) from Merck, *n*-heptane (99%) and acetophenone (99%) from Acros, chloroform from Labscan Ltd., sodium chloride (99.9%) from Akzo Nobel and dichloromethane (99.95%) and toluene (99.7%) from Chemproha. 3,5-Dinitrobenzoyl-D,L-leucine and *O*-(1-*t*-butylcarbamoyl)-11-octadecylsulfinyl-10,11-dihydro-quinine were kindly provided by DSM Research. An overview of the solvents with their properties relevant to the presented studies is given in Table 2.

### 3.2. Equipment and procedures

In all operations where the temperature is mentioned, the temperature was measured at the inlet and the outlet of the CINC. By using tap water for cooling the outlet temperature could be kept constant at 294 K, the same temperature of the liquids entering. Similarly, if a higher temperature was desired, the temperature could be controlled using a water bath.

#### 3.2.1. Liquid hold-ups

The liquid hold-up determinations were carried out in a stainless steel CINC V02 obtained from CINC Industries (Carson City, Nevada, USA). The V02 is a table-top version with a maximum total throughput of 1.9 L/min and a maximum rotational frequency of 100 Hz. Both liquids were transferred to the device using Verder VL1000 Control peristaltic tube pumps equipped with double pump heads ($1.6 \times 1.6 \times 8$R). The supply and receive vessels (2–3 L volume typically) were made of glass. The total liquid hold-ups of both phases in the device were determined using 4 Mettler PM4000 balances connected to a PC. The mass of the supply and receive vessels were monitored using Labview® software (National Instruments). The experiments were performed at $293 < T < 318$ K in the low-mix configuration (Fig. 1B). A measurement was initiated by starting the rotor and the pumps. The total hold-ups were obtained from the weight measurements of the supply and receive vessels. By subtracting the steady-state hold-up in the tubes from the measured values, the actual hold-up in the device could be determined. The steady-state hold-up in the tubes were obtained from the RTD measurements (vide infra).

The hold-ups in the centrifuge and the annular zone were determined by performing experiments with a preselected solvent combination (water with heptane, octanol, toluene, DCE, DCM, or chloroform). An experiment was started by feeding the two liquids to the CCS device. After reaching steady state (about four residence times), the pumps were shut down and the annular volume was drained by opening the valve in the bottom of the annular zone. The volumes of both phases were determined using a measuring cylinder. Subsequently, the centrifuge was stopped and the remaining liquid in the centrifuge was drained. The volumes of both phases were determined using a measuring cylinder. Measurements were performed for all three configurations (Fig. 1).

#### 3.2.2. RTD experiments

The RTD measurements were carried out with the CINC V02. The aqueous reactor inlet and outlet were equipped with conductivity cells (Vernier) connected to a PC via a Coachlab II (CMA) interface, the organic phase inlet and outlet with 2 S8D31D UV LED's (Roithner-lasertechnik) and monitored using UVB-sensors (Vernier). The RTD curves were determined for four different CCS configurations, by applying different sizes of tubes in several experiments, it was verified that the RTD signal was under the studied conditions not measurably affected by the contractions/enlargements in the reactor inlet and outlet. In the standard configuration (high mix), the liquids enter on the sides as depicted in Fig. 1A and are in direct contact with the rotating centrifuge. In the "low-mix" configuration, the rotating centrifuge is shielded for the entering liquids (Fig. 1B). In the other two configurations, either the aqueous phase or the organic phase is fed via a tube through the bottom hole directly into the centrifuge (Fig. 1C). An experiment was started by feeding the liquids to the CINC and the device was allowed to reach steady state (four average residence times, vide infra). The RTD curves were determined at 294 K by measuring the response to a step function of tracer in the inlet. Flow rates were varied from 20 to 50 mL/min per phase, the rotational frequency

**Table 2**
Solvent properties at 25 °C of used solvents and applied heavy phase weirs [35].

| Solvent | Density (kg/m$^3$) | Weir applied (mm) | Viscosity (mPa s) | Interfacial tension with water (mN/m) |
|---|---|---|---|---|
| Water | 997 | [–] | 0.890 | [–] |
| Heptane | 684 | 26.67 | 0.387 | 51.7 [36] |
| Toluene | 865 | 23.50 | 0.560 | 35.7 [37] |
| Dichloromethane | 1325 | 25.40 | 0.413 | 27 [38] |
| 1,2-Dichloroethane | 1256 | 24.77 | 0.779 | 23 [39] |
| Chloroform | 1492 | 26.67 | 0.537 | 23.0 [37] |
| 1-octanol | 827 | 24.13 | 3.232 | 8.19 [40] |

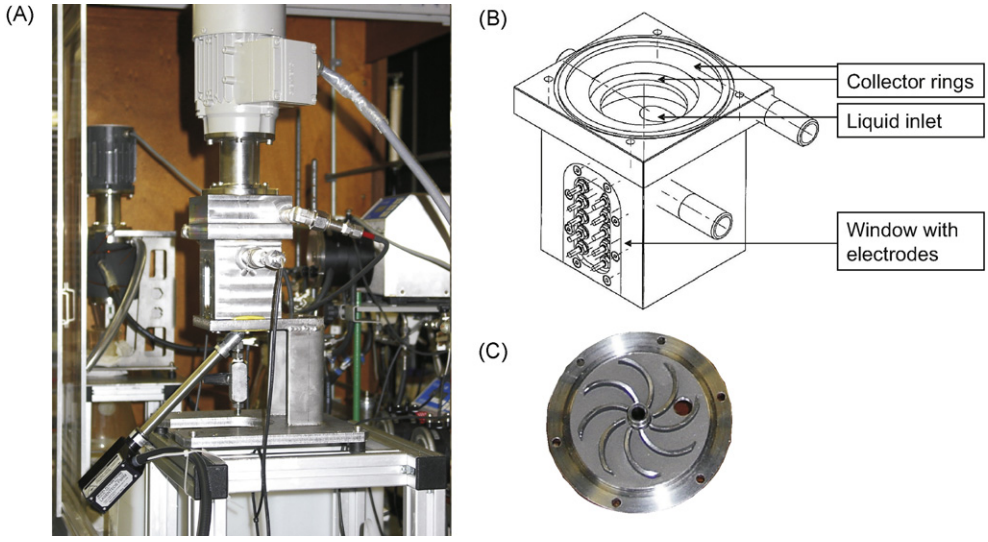


**Fig. 3.** (A) Photograph of the CS50 showing the position of the tip of the FBRM probe in the bottom plate, (B) drawing of the non-rotating reactor house, and (C) picture of the original high-mix bottom plate with extra hole. The extra hole on the right was adjusted so that the probe could be mounted.

from 30 to 60 Hz. For the aqueous phase, NaCl (typically 15 g/L) was used as the tracer. For the organic phase acetophenone (typically 0.3–2 vol%, depending on the solvent) was used. The step responses were measured every 0.33 s using UV absorbance (organic phase) and conductivity (aqueous phase). For a series of measurements using toluene as solvent (13–22 in Table 1), the step responses were measured four times to check the reproducibility. Also, the CINC was stopped after every measurement to determine annular and centrifugal volumes (*vide infra*). Other measurements were done in duplo by a combined "step up" and a "step down".

The experimentally obtained step responses at the inlets and outlets of the CINC were normalized and the step response of the device was then obtained by correcting the outlet signal for the delayed inlet signals. For fitting of the mixers-in-series based models on the averaged experimental responses the mean relative error (MRE) was used as criterion.

$$\mathrm{MRE} = \frac{\sum_{n=1}^{N} \left(F_{\mathrm{exp},n} - F_{\mathrm{mod},n}\right) / F_{\mathrm{exp},n}}{N} \times 100\%. \quad (4)$$

To circumvent that huge errors at very small values of the responses just after the step was applied dominate the fitting procedure, the time interval was set at $0.5 < t < 25$.

### 3.2.3. Drop size distributions

For determination of the drop size distributions a CS50 equipped with a Perspex window obtained from CINC Solutions (Doetinchem, The Netherlands) was used. The internal geometry of the CS50 is identical to that of the CINC V02 (Fig. 3). for more details. The drop size distributions were determined with Lasentec® S400A focused beam reflectance measurement (FBRM) equipment with a PI 14/206 probe (Mettler Toledo). The tip of the probe was positioned between the vanes of the high mix bottom plate under an angle of 45°, pointing into the direction of the flow (Fig. 3). The diameter of the tip of the probe is 8 mm, having a perfect fit in between the bottom plate and the rotor with its 5.7 mm height under a 45° angle. The vanes are 5 mm high and the space between the bottom plate and the rotor is 7 mm.

The FBRM uses laser light to measure the reflectance of drops and converts this to chord size distributions. The chord size distributions were corrected to actual droplet size distributions by applying a correction factor. For perfectly spherical droplets and assuming that the system is well mixed [29], the average chord size is 79% of the average droplet size (as indicated by the manufacturer). Measurements were done at 294 K at steady state, flow rates were varied from 10 to 50 mL/min per phase, and the rotational frequency from 30 to 50 Hz.

### 3.2.4. Conductivity measurements to determine the continuous and dispersed phase

A modified CS50 with a perspex window was used for determination of the continuous and dispersed phase. The perspex window was equipped with copper electrodes. An electronic circuit with a 10 V potential was connected to the two lowest copper electrodes and a 10 kΩ resistance in series. The partial resistance over the liquid in the annular zone of the CCS was measured using a voltmeter connected to a PC via a Coachlab II interface (CMA). The experiments were carried out at 294 K at steady state, flow rates were varied from 20 to 80 mL/min per phase and the rotational frequency from 30 to 50 Hz.

## 4. Results and discussion

The maximum liquid throughput of the CCS device applied in this study is 1.9 L/min (vendor information). For the applications of our interest (biphasic catalysis and reactive extractions) typically relatively low flow rates (<100 mL/min total flow) are applied to allow for sufficient residence times to achieve high conversions. Therefore, all experimental results presented in this paper were determined in this relatively low flow regime. All systems described here are aqueous–organic biphasic systems.

### 4.1. Determination of the liquid hold-ups

The total liquid hold-up ($V_{\mathrm{L,tot.}} = V_{\mathrm{org,tot}} + V_{\mathrm{aq,tot}}$) in the CCS device as well as the total liquid hold-up of the individual phases ($V_{\mathrm{org,tot}}$, $V_{\mathrm{aq,tot}}$) were determined gravimetrically by continuously monitoring the weights of supply and receive vessels during an experiment. The liquid hold-ups in the centrifuge ($V_{\mathrm{CENTR}} = V_{\mathrm{aq,CENTR}} + V_{\mathrm{org,CENTR}}$) were determined using a different method involving a special shut-down procedure. The gravimetrical determination was carried out for a water–heptane system, the centrifugal liquid hold-ups were determined for a range of

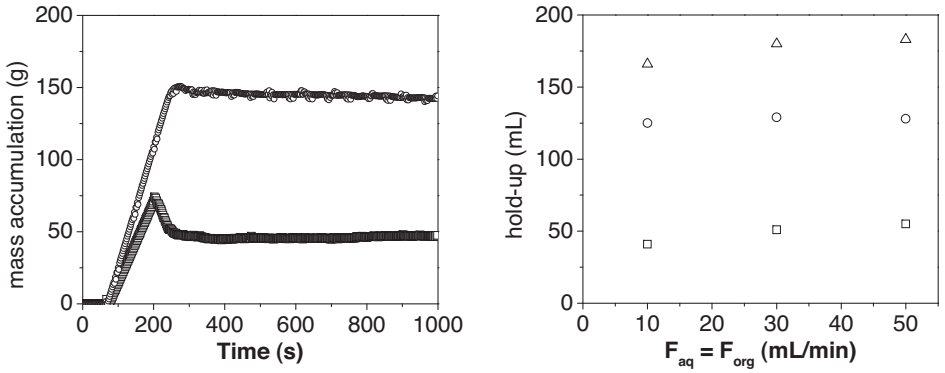


**Fig. 4.** Left: Mass accumulation in the system as function of time, determined by gravimetry. Settings: Org = heptane, $F_{org} = F_{aq} = 50$ mL/min, $\upsilon = 30$ Hz, low-mix configuration. Symbols: □ = heptane mass (g), ○ = water mass (g). Right: steady state hold-up determined from gravimetric mass accumulation for varying $F_{org} = F_{aq}$. Settings: Settings: Org = heptane, $\upsilon = 30$ Hz, low-mix configuration. Symbols: □ = heptane volume (mL), ○ = water volume (mL), △ = total volume (mL).

water–organic solvent combinations (i.e. heptane, toluene, octanol, DCE, DCM, and chloroform).

#### 4.1.1. Gravimetric determination of the total liquid hold-ups for heptane–water system

The total liquid hold-up for the heptane–water system as a function of rotor speed and liquid throughputs were determined at $293 < T < 318$ K in the low-mix configuration (Fig. 1B) by weight measurement of the supply and receive vessels. The flow rates were varied from 10 mL/min each to 50 mL/min each and the rotational frequency was varied from 30 to 60 Hz.

In a typical experiment using heptane and water in the low-mix mode operated at 50 mL/min flows and 30 Hz the pumps were started simultaneously. As soon as the pumps were started, the mass started to accumulate in the system (see Fig. 4 (left) for the accumulation graph). Initially, the accumulation is linearly, the slope of heptane being lower because of the lower density. After about 200 s, the rate of heptane accumulation suddenly becomes negative, implying that more heptane is leaving the system than entering. This is because the heavier water is displacing the heptane in the centrifuge. After about 300 s the accumulation in the system is at steady state.

It follows from Fig. 4 (right) that the total steady-state liquid hold-up varied between 160 mL (30 Hz, 10 mL/min for both phases) to 178 mL (30 Hz, 50 mL/min for both phases). The geometrical volume of the device is 322 mL and thus it may be concluded that about half of the device is filled with liquid, the remainder being air. This air is located in the center of the centrifuge (which is logical in a centrifugal operation), but also partly in the annular zone that apparently is filled only for a small portion.

The total aqueous phase hold-up ranged from 119 mL to 123 mL at 10 and 50 mL/min flow per phase, respectively. These values are considerably higher than the heptane hold-up (41–55 mL). Furthermore, it may be concluded that the flow rate of each phase only has a very small effect on the total liquid hold-ups in the device.

To gain insights in this surprisingly small effect of the flow rates on the total liquid hold-up, the liquid hold-ups in the centrifuge were determined as a function of the flow rates.

#### 4.1.2. Liquid hold-ups in the centrifuge and the annular zone of the CCS device

The liquid hold-up in the centrifuge ($V_{CENTR} = V_{aq,CENTR} + V_{org,CENTR}$) and the annular zone were determined for a number of aqueous–organic solvent systems (heptane, toluene, DCE, DCM, chloroform and octanol). The hold-ups in the centrifuge were determined for both the high mix and low-mix configuration. An experiment in the CINC was initiated with the pre-determined settings and allowed to reach steady state. Subsequently, the pumps were stopped and the liquids were purged from the annular zone. After purging the annular zone the centrifuge was stopped and the liquids from the centrifuge purged, collected and measured. A diagram displaying the results for toluene–water in the high mix setup is displayed in Fig. 5.

From Fig. 5 it may be concluded that the volumes determined by purging of the system tend to be rather constant ($V_{aq,CENTR}$ typically 90–100 mL, $V_{org,CENTR}$ 60–70 mL, and $V_{aq,ANN}$ and $V_{org,ANN}$ both about 5 mL), but with deviations. No logic was found in the occurrence of the deviations. For any of the solvents, the annular volume was found to be mostly about 5 mL per phase, but deviations were observed up to 25 mL per phase, especially when using heptane in the low-mix configuration. The cause of these deviations is unclear. For the centrifugal volume, much less deviations were observed and the hold-ups of the aqueous and organic phase were found to total always about 170 mL with a ratio that is dependent on the selected weir. At the applied operating regime using relatively low flows, the hold-up ratios are thus governed by geometric factors due to the high centrifugal forces in the centrifuge. An overview of the modal centrifugal volume for a range of solvents is presented

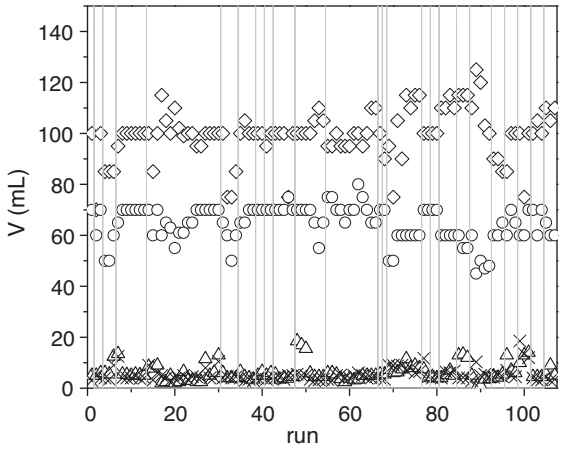


**Fig. 5.** Hold-up determination in the annular zone and the centrifuge for toluene–water in the high-mix setup under various conditions. Notation for $F_{aq} = 30$ mL/min, $F_{org} = 30$ mL/min, and $\upsilon = 30$ Hz: 30/30/30. Run 1: 10/10/60, Run 2–3: 15/15/60, Run 4–6: 20/20/60, run 7–13: 25/25/60, Run 14–30: 30/30/60, Run 31–34: 50/50/60, Run 35–38: 100/100/60, Run 39–40: 50/30/60, Run 41–42: 30/50/60, Run 43–47: 30/100/60, Run 48–54: 100/30/60, Run 55–66: 30/30/50, Run 67: 30/30/70, Run 68: 30/30/90, Run 69–76: 30/30/40, Run 77–80: 30/50/50, Run 81–84: 30/100/40, Run 85–87: 100/30/40, Run 88–92: 50/50/40, Run 93–95: 50/50/50, Run 96–98: 50/30/50, Run 99–101: 50/100/50, Run 102–104: 100/50/50, Run 105–107: 100/100/40. Symbols: ◊: $V_{aq,CENTR}$, ○: $V_{org,CENTR}$, △: $V_{aq,ANN}$, ×: $V_{org,ANN}$. Vertical lines separate runs with different settings.

**Table 3**
Measured $V_{CENTR}$ for various aqueous–organic systems.

| Organic solvent | Weir size (mm) | $V_{aq,CENTR}$ (mL)[a] | $V_{org,CENTR}$ (mL) | $V_{total,\ CENTR}$ (mL) |
|---|---|---|---|---|
| Heptane[b] | 26.67 | 120–130 | 40–50 | 165–175 |
| Octanol[b] | 24.13 | 100–110 | 60–70 | 165–175 |
| Toluene[b] | 23.50 | 90–100 | 70–80 | 165–175 |
| DCE[c] | 24.77 | 80–90 | 80–90 | 165–175 |
| DCM[c] | 25.40 | 70–80 | 90–100 | 165–175 |
| Chloroform[c] | 26.67 | 65–75 | 90–100 | 165–175 |

[a] $V_{CENTR}$ was determined at 294 K for flow rates up to 100 mL/min per phase.
[b] Organic phase lighter than water.
[c] Organic phase heavier than water.

in Table 3.The small annular hold-ups were confirmed by visual observations using the CS50 equipped with a transparent perspex window. Within the range of experimental settings of flow rate and rotor speed, the liquid level in the annular zone was always just above the bottom of the centrifuge. Apparently in the operational regime of <100 mL/min flow per phase, the pump action of the rotating centrifuge is rather high and leads to low liquid volumes in the annular zone.

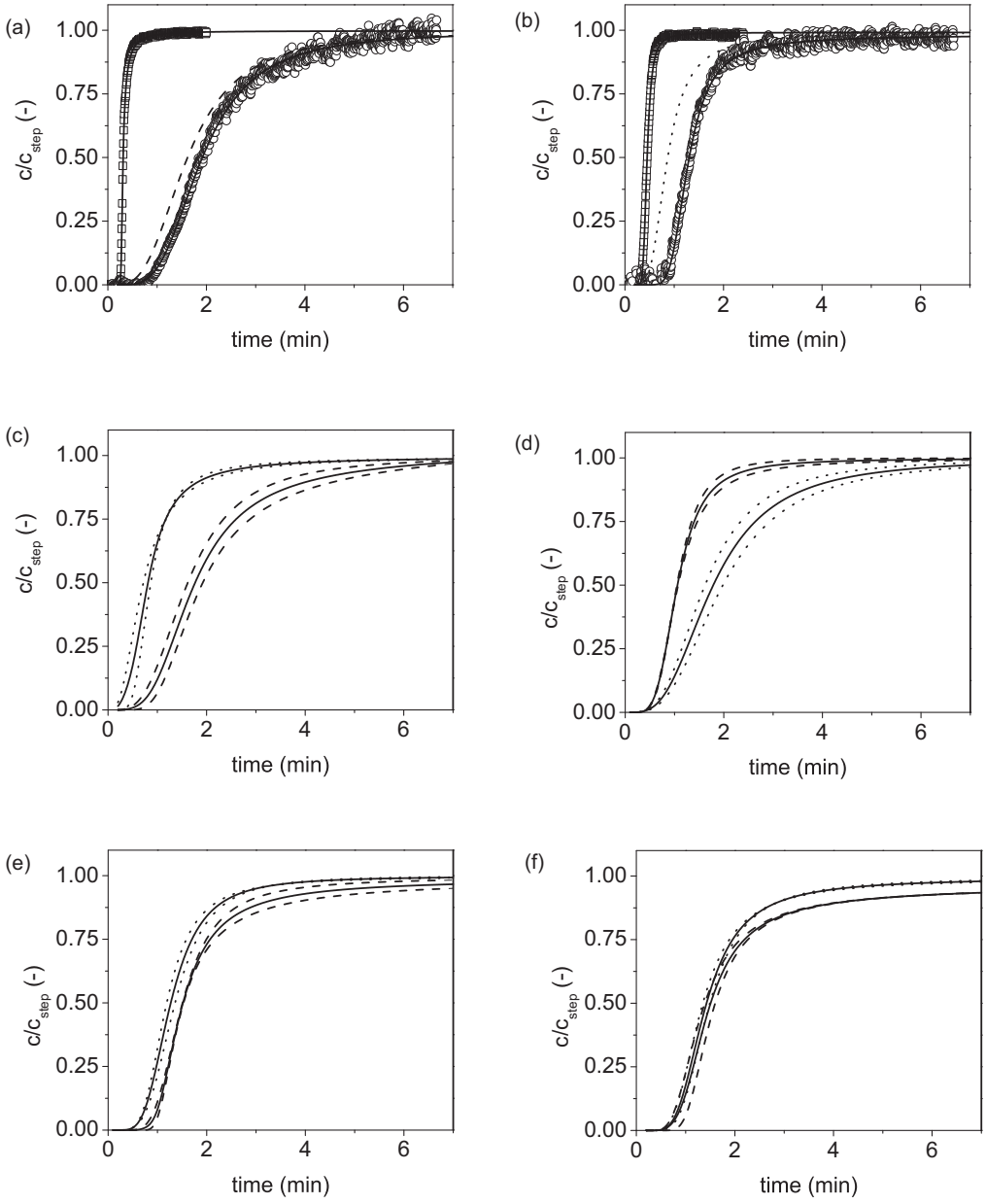


**Fig. 6.** RTD responses at $F_{aq} = F_{org} = 50$ mL/min and $\upsilon = 30$ Hz. (a) and (b): experimental inlet (□) and outlet (○) response curves for water–toluene system in high mix configuration, dashed lines: the corrected CINC responses, (a) = water response; (b) = toluene response; (c)–(f): corrected reactor responses. Dashed lines: aqueous response, dotted lines: organic response, solid lines: average response from duplo measurements. (c) Exp. 23 Table 4: water(h)–toluene(l), high mix; (d) Exp. 25 Table 3: water(l)–DCE(h), high mix; (e) Exp. 24 Table 4: water(h)–octanol(l), high mix; (f) Exp. 10 Table 3: water(h)–heptane(l), low mix.

**Table 4**
Residence time distribution settings and modeling results.

| Experimental settings | | | | | | Modeling results[a] | | | | | | | | | |
|---|---|---|---|---|---|---|---|---|---|---|---|---|---|---|---|
| Exp. | Organic solvent | $F_{aq}$ (mL/min) | $F_{org}$ (mL/min) | $\upsilon$ (Hz) | Configuration | $V_{aq}$ (mL) | $V_{org}$ (mL) | $N_{aq}$ (−) | $V_{dead,aq}$ (mL) | $\phi_{v,d,aq}$ (mL/min) | MRE[b] (%) | $N_{org}$ (−) | $V_{dead,org}$ (mL) | $\phi_{v,d,org}$ (mL/min) | MRE[b] (%) |
| 1[c] | Heptane | 20 | 20 | 30 | LM | 102 | 59 | 9 | 43 | 15 | 8.66 | 11 | 22 | 0.0058 | 5.50 |
| 2[c] | Heptane | 20 | 20 | 40 | LM | 105 | 93 | 6 | 20 | 0.6 | 7.61 | 25 | 15 | 0.0036 | 7.47 |
| 3 | Heptane | 30 | 30 | 40 | LM | 97 | 82 | 5 | 17 | 2.22 | 0.087 | 14 | 23 | 0.09 | 3.88 |
| 4 | Heptane | 30 | 30 | 50 | LM | 101 | 95 | 6 | 22 | 0.1 | 2.91 | 18 | 15 | 0.036 | 4.11 |
| 5 | Heptane | 30 | 30 | 60 | LM | 91 | 81 | 6 | 21 | 3 | 3.15 | 31 | 16 | 0.006 | 3.69 |
| 6 | Heptane | 40 | 40 | 30 | LM | 108 | 60 | 6 | 15 | 2 | 2.16 | 25 | 26 | 0.0048 | 3.77 |
| 7 | Heptane | 40 | 40 | 40 | LM | 109 | 79 | 7 | 17 | 0.4 | 2.58 | 38 | 12 | 0.016 | 6.28 |
| 8 | Heptane | 40 | 40 | 50 | LM | 108 | 91 | 8 | 39 | 20 | 4.60 | 23 | 7 | 0.0084 | 7.62 |
| 9 | Heptane | 40 | 40 | 60 | LM | 110 | 85 | 9 | 45 | 13 | 9.14 | 42 | 24 | 0.081 | 5.55 |
| 10 | Heptane | 50 | 50 | 30 | LM | 103 | 91 | 7 | 25 | 11.25 | 7.14 | 7 | 24 | 2.50 | 4.50 |
| 11 | Heptane | 50 | 50 | 40 | LM | 92 | 93 | 28 | 55 | 192 | 3.95 | 15 | 11 | 0.035 | 5.91 |
| 12 | Heptane | 50 | 50 | 50 | LM | 93 | 98 | 5 | 43 | 17.5 | 5.57 | 6 | 38 | 0.15 | 3.24 |
| 13 | Toluene | 30 | 30 | 40 | LM | 76 | 73 | 8 | 20 | 0.3 | 2.36 | 5 | 15 | 0.063 | 2.22 |
| 14 | Toluene | 30 | 30 | 50 | LM | 75 | 67 | 7 | 20 | 0.75 | 2.18 | 7 | 14 | 0.243 | 5.16 |
| 15 | Toluene | 30 | 30 | 60 | LM | 82 | 73 | 8 | 20 | 0.6 | 2.55 | 6 | 16 | 2.25 | 5.07 |
| 16 | Toluene | 30 | 30 | 40 | AQBF | 71 | 74 | 8 | 20 | 0.75 | 2.24 | 7 | 18 | 0.123 | 2.39 |
| 17 | Toluene | 30 | 30 | 60 | AQBF | 61 | 84 | 9 | 27 | 4.5 | 3.10 | 8 | 15 | 0.303 | 6.21 |
| 18 | Toluene | 30 | 30 | 40 | ORGBF | 79 | 65 | 9 | 22 | 0.6 | 2.47 | 5 | 20 | 0.213 | 1.90 |
| 19 | Toluene | 30 | 30 | 60 | ORGBF | 82 | 64 | 9 | 18 | 0.9 | 3.11 | 5 | 21 | 0.393 | 2.13 |
| 20 | Toluene | 30 | 30 | 40 | HM | 97 | 89 | 7 | 24 | 2.25 | 3.05 | 6 | 19 | 0.15 | 2.62 |
| 21 | Toluene | 30 | 30 | 50 | HM | 91 | 85 | 9 | 28 | 5.25 | 3.11 | 7 | 15 | 1.5 | 5.88 |
| 22 | Toluene | 30 | 30 | 60 | HM | 88 | 90 | 6 | 20 | 1.5 | 2.43 | 7 | 23 | 3.0 | 5.46 |
| 23[d] | Toluene | 50 | 50 | 30 | HM | 113 | 55 | 5 | 29 | 6.42 | 2.03 | 5 | 17 | 2.67 | 2.23 |
| 24[d] | Octanol | 50 | 50 | 30 | HM | 100 | 76 | 12 | 59 | 32.7 | 4.34 | 6 | 20 | 1.67 | 1.45 |
| 25[e] | DCE[f] | 50 | 50 | 30 | HM | 63 | 114 | 7 | 13 | 3.92 | 1.64 | 5 | 17 | 3.92 | 1.32 |

[a] To avoid too many model parameters, the annular volume was fixed at 5 mL. This fixation seems a reasonable estimate (*vide infra*). The model was run with varying annular volume to check the dependency on the annular volume. In general, with a different annular volume a different dead zone and a different exchange rate was found, but the goodness of fit was comparable.

[b] The MRE is the mean relative error, defined in Eq. (4).

[c] The time interval for the fitting was started at 0.85 min, instead of the usual 0.5 min.

[d] Time interval for the fitting was started at 0.25 min, instead of the usual 0.5 min.

[e] Time interval for the fitting was started at 0.10 min, instead of the usual 0.5 min.

[f] In the DCE–water system the organic phase is the heavy phase.

### 4.2. Residence time distributions

RTD curves for both liquid phases (water–organic) in the CCS were determined experimentally for water in combination with toluene, heptane, DCE, and octanol by measuring the response of a step input. Responses of both phases in typical experiments at $F_{aq} = F_{org} = 50$ mL/min and $\upsilon = 30$ Hz are displayed in Fig. 6.

The graphs in Fig. 6a and b correspond to single experiments, and the corrected CINC V02 response function. The other graphs in Fig. 6c–f show duplicate corrected CINC V02 response runs with their averaged response ($C(t) = (C_1(t) + C_2(2))/2$). It follows from Fig. 6 that the duplicate runs are in good accordance, but to obtain more information on the repeatability a series of experiments was repeated four times (Exp. 13–22, Table 4). From the individual responses the first moment of the RTD (mean time) was calculated. The average 95% confidence limit error in the first moment is 9%, an expectable error for series of four repetitions. The main conclusion that can be drawn from the responses displayed in Fig. 6 is that independent of the liquids used, the response curves always tail to some extent. The tailing suggests a dead zone, the fluids apparently pass through a stagnant zone. This stagnant zone may be located in the upper part of the centrifuge close to the interface, but also the hold-up in the collector rings may be short-cutted close to the outlet, leaving large parts of the rings as dead zones.

Because of the tailing, the standard tanks-in-series model does not fit satisfactorily. Therefore, the RTD responses were modeled using a tanks-in-series model extended with a dead-volume zone (Fig. 2). Before explaining the details of this model the unsatisfactory fitting of the regular tanks-in-series model is illustrated in Fig. 7. The MRE (mean relative error, Eq. (4)) is displayed as function of the number of tanks in Fig. 7a. Also, the best fits using the standard tanks-in-series model (with $N = 3$) and the derived model with a dead zone are compared in Fig. 7b. It is clear that the dead-zone model fits better. An overview of all RTD results is given in Table 4.

Several conclusions follow from Table 4. First, the number of mixers is generally (with a few exceptions, Exp. 11, 22, and 24) higher for the dispersed phase than for the continuous phase. This indicates that less back-mixing is observed for the dispersed phase than for the continuous phase. Second, the volume of the dead zone is typically around 20 mL for both the aqueous phase and the organic phase. For the heavy phase, this could correspond with a film on the centrifuge wall of about 1.5 mm thickness, whereas at the light side of the interface the thickness of the film should be almost 5 mm over the entire height of the centrifuge to achieve. A film of 5 mm thickness appears not so realistic, supporting our suggestion that the collector rings behave as a dead zone as well.

Comparing the total hold-up determined by RTD and by the experimental determination described in Section 4.1, it may be concluded that the comparison is reasonable. For example, for heptane–water under identical conditions (30 Hz, $F_{aq} = F_{org} = 40$ mL/min, low mix) the total volume of the aqueous phase in the CCS was 108 mL according to RTD measurements versus 120 mL for the flow experiments. The volume of the organic phase in the CCS was 60 mL according to the RTD calculations versus 55 mL for the flow measurements. However, in some cases the volumes deviate significantly. The deviations may arise from the uncertainty in the experimental procedure. Examining Fig. 6a and b, it is clear that the error in the concentration measurement at the outlet of the reactor can be as much as 10%. This does not affect the fitting of the number of tanks in series too much because the MRE was used as criterion (Eq. 4). The volume determination can though be affected quite significantly when a tailing curve is fitted slightly different. It may be concluded from this study that the RTD of the flows through the CCS are described well using a tanks-in-series model with a dead zone (Fig. 2). Typically for the flow that forms the continuous phase the RTD is described by about seven tanks in series with a 20 mL dead zone. For the flow that forms the dispersed phase, usually eight or more tanks with a 20 mL dead zone fit the corrected response function well. For multiphase reaction engineering purposes, these figures may be used, if also information on the interfacial area of that specific system is known. Therefore, information on the drop sizes is pursued in the next section.

### 4.3. Drop size distribution

The drop size distribution of the dispersed phase in the annular zone was determined at a fixed temperature (294 K) for various process conditions (flow ratios, rotational frequency, solute(s)) using FBRM technology. The studies were performed for three different aqueous–organic solvent systems (heptane, toluene and DCE). In general, the most frequently occurring drops were found to be smaller than 50 μ, indicating that the annular zone is well mixed, in accordance with previously reported CFD studies [26].

#### 4.3.1. Effect of the flow ratio on the mean drop size

The effect of the flow ratio on the drop size distribution was studied at 30 Hz for a biphasic system consisting of DCE–water. Starting with equal flow rates (50 mL/min), the DCE flow was step wise reduced to 20 mL/min while maintaining a constant water flow rate of 50 mL/min. After a disturbance, the system was allowed to attain steady state. Subsequently, the sequence was reversed and the DCE flow was stepwise increased again to 50 mL/min. Fig. 8 displays the measured $\overline{d_{vs}}$ at varying DCE flow rate. The $\overline{d_{vs}}$ increased slightly but gradually with decreasing DCE flow from

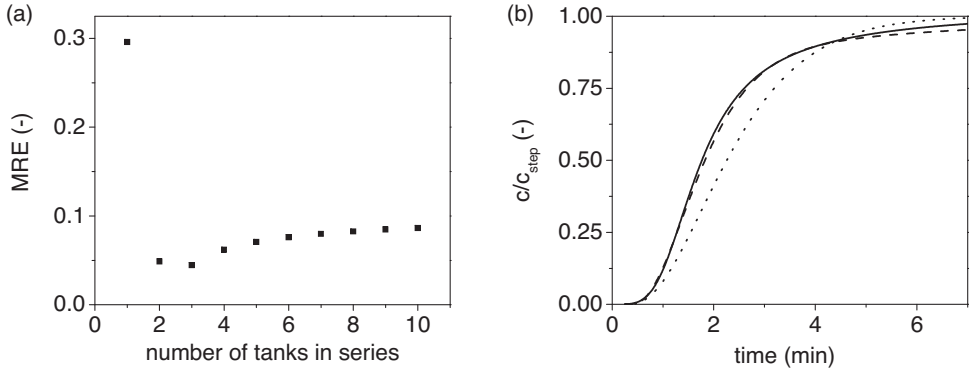


**Fig. 7.** (a) MRE (fraction) of tanks-in-series model fit to deconvoluted aqueous phase response for the experiment in Fig. 6a (Exp. 23 Table 4, $F_{aq} = F_{org} = 50$ mL/min and $\upsilon = 30$ Hz, toluene–water, HM) (b) The actual response curves for Exp. 23. Solid: averaged corrected response (see also Fig. 6c), dashed: best fit using tanks-in-series model with dead zone (see Table 4 for conditions), dotted: best fit standard tanks-in-series model (three tanks).

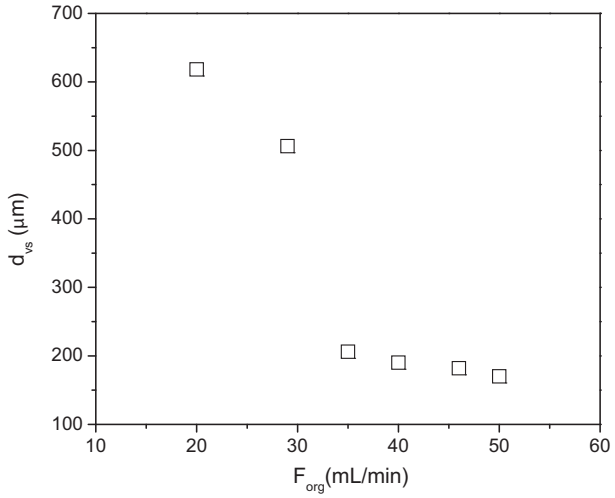


**Fig. 8.** Sauter mean drop size for pure DCE and water as a function of the organic flow rate ($F_{aq}$ = 50 mL/min, $\upsilon$ = 30 Hz).

50 till 29 mL/min. At this value (corresponding to a flow ratio $F_{org}/F_{aq}$ = 0.58) the Sauter mean drop size suddenly increases dramatically. This increase is due to phase inversion (vide infra). When increasing the flow rate again, the same sudden change in drop size was again found at 29 mL/min. Such dramatic changes in drop sizes upon phase inversion were also reported by Van Woezik and Westerterp [41] for the system butyl formate and sodium hydroxide.

*4.3.2. Effect of rotational frequency on the specific interfacial area*

For the water–DCE system, the effect of the rotational frequency on the drop size distribution could not be measured due to substantial entrainment of air bubbles above 30 Hz. These air bubbles disturbed the measurements considerably and do not allow for a proper calculation of the Sauter mean drop sizes. Better results were obtained with a system used for enantioselective liquid–liquid extraction of 3,5-dinitrobenzoyl-*(R)*,*(S)*-Leucine (DNB-leu) [15]. Here, the aqueous phase contains a phosphate buffer and DNB-leu, and the DCE phase is loaded with a cinchona alkaloid extractant (C). With this liquid–liquid system, air entrainment was not observed for 30 Hz < $\upsilon$ < 50 Hz. Fig. 9 shows the experimental drop size distributions at different rotational frequencies.

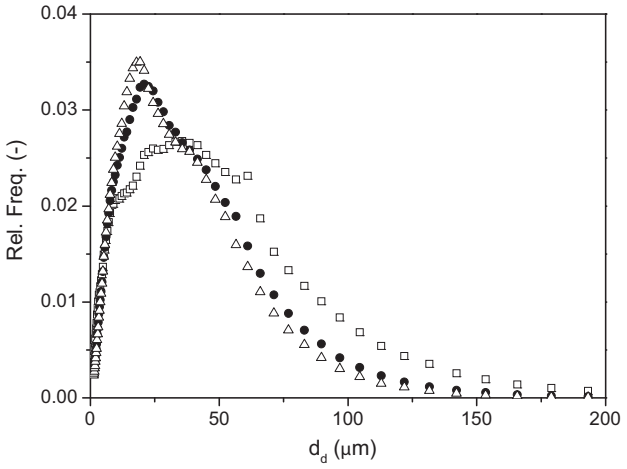


**Fig. 9.** Drop size distributions at various rotational frequencies for DCE–water system containing $1 \times 10^{-3}$ mol/L DNB-leu (aq) and $3 \times 10^{-4}$ mol/L C (org). Flow rates: 50 mL/min water phase and 50 mL/min DCE phase. Symbols: △ = 50 Hz, ● = 40 Hz, □ = 30 Hz.

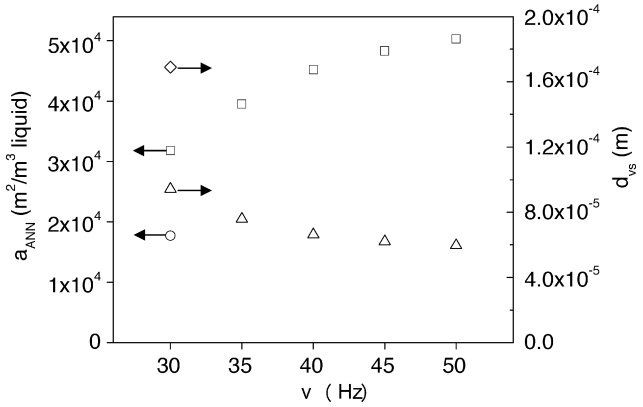


**Fig. 10.** Specific interfacial area and Sauter mean drop size in the annular zone for the system DCE–water at 50 mL/min for both flows. Symbols: ◯ and ◊ pure DCE and water, □ and △: DCE and water with the solutes DNB-leu and C.

It is clear that at higher rotational frequencies the number of small drops increases and the number of large drops decreases. Thus, higher power inputs lead to lower drop sizes.

The specific interfacial area for each experiment was calculated using Eqs. (2) and (3). Here, the Sauter mean drop size was obtained from the FBRM measurements. Furthermore, it was assumed that the hold-up ratio of both liquid phases in the annular zone is equal to the flow ratio, allowing calculation of $\varepsilon$. This assumption was shown to be valid for well-mixed vessels [30]. The resulting interfacial areas are displayed in Fig. 10 for the DCE–water system with solutes DNB-leu and C at a series of rotational frequencies.

It may be concluded that the specific interfacial area in the annular zone exceeds the values of $10^2$–$10^4$ $m^2/(m^3$ liquid) typically observed in stirred tank vessels [41,42] for all rotor frequencies. The specific area increases with increasing rotor speeds and highest values were observed at 50 Hz. However, the curve appears to level off, suggesting that above a certain, yet unknown, rotational frequency the drop size distribution becomes independent of the rotational frequency. Leveling off of the drop size distribution dependency on rotational frequency is due to a dynamic equilibrium between coalescence and breakage occurring. This upper limit could unfortunately not be determined experimentally as air bubbles were struck in the dispersion above 50 Hz and disturbed the measurements.

For the system pure DCE and water the interfacial area could only be obtained at 30 Hz. Values at higher frequencies were unreliable due to considerable amounts of air bubbles in the system. The specific annular interfacial area for pure DCE–water is about a factor of two lower than the values in the presence of solutes. This is likely caused by surface activity of the solutes [31]. Surface active components are known to reduce the interfacial tension, leading to smaller drops and a higher specific interfacial area.

Comparing the specific interfacial areas of about six times higher than in stirred tanks from this study with the total interfacial area being about the area in stirred tanks in a previous study [20] suggests that for modeling interphase mass transport and chemical reaction engineering using the RTD model from the previous section the mass transfer could take place in the annular zone and in the first tank from the series describing the centrifuge. This hypothesis will be studied in more detail and system specifically in our upcoming paper on enzyme catalyzed conversion in the CCS.

*4.4. Phase behavior*

For a number of aqueous–organic (DCE, DCM, chloroform, octanol, heptane and toluene) biphasic systems the continuous phase was determined using conductivity measurements as

**Table 5**
Inversion conditions for aqueous–organic biphasic systems.

| Organic solvent | $\upsilon$ (Hz) | $F_{aq}$ (mL/min) | $F_{org}$ (mL/min) |
|---|---|---|---|
| Octanol | 50 | 20 | 40 |
| DCE | 30 | 50 | 29 |
| DCM | 30 | 20 | 80 |
| DCM | 50 | 30 | 30 |

described in Section 3 at 294 K and a range of flow rates and rotational frequencies.

For toluene–water, toluene was the continuous phase over the entire operating window ($0.25 < R = F_{org}/F_{aq} < 4$, and $30 < \upsilon < 50$), while *n*-heptane and chloroform were always the disperse phase. For DCM, DCE and 1-octanol phase inversion was observed in the operating window. At high values of $R = F_{org}/F_{aq}$, the organic phase was continuous whereas the opposite was observed at low values of R. The conditions at the inversion points are listed in Table 5.

From the DCM measurements it can be concluded that phase inversion is depending on the rotational frequency, as for DCM inversion from a continuous aqueous phase to a continuous organic phase takes place at a lower flow ratio (org/aq) at higher rotational frequency, i.e. higher power input. This observation is in line with the results of Liu et al. [34].

## 5. Conclusions

We have determined information on liquid hold-up, residence time distribution, drop size distribution in the annular zone, and dispersed phase in the annular zone for the CINC V02 (and the equivalent CS50) under various operating conditions (flow rates and ratios and rotor speeds) for a number of water–organic solvent systems.

The total liquid hold-up fraction in the CCS is about 0.5, the remainder being air. Most of the liquid resides in the centrifuge and the annular zone is only partly filled with liquids (about 10 mL for the settings in this study). The liquid distribution in the annular zone and the centrifuge is a function of the physical properties of the solvents, the phase with the highest density is present in the highest amounts, and the density difference determines the choice of weir and with that affects the hold-up ratio. RTD measurements indicate that the overall macro-mixing behavior of both phases is close to plug flow and is heavily dominated by the centrifuge. Tailing indicates a dead zone. The RTD measurements were fitted to a tanks-in-series model with a dead zone. The best fits were obtained with a dead zone of about 20 mL per phase, and about seven tanks in series for the continuous phase and eight or more tanks in series for the dispersed phase. The specific interfacial area in the annular zone was determined using a laser probe and was up to 50.000 $m^2/m^3_{liq}$ at 50 Hz rotor speed which is typically 6–10 times higher than typically reported for stirred vessels. Comparing this high specific interfacial area with the previously determined total interfacial area suggests that under the investigated conditions (low flows) for mass transfer operations only the annular zone and the lower part of the centrifuge are effective. In the RTD model this corresponds to the annular zone and the first tank in the series describing the centrifuge. This hypothesis will be tested in follow-up studies on specific systems, such as biphasic enzyme reactions in the CCS.

The data are currently used for reactor modeling of biphasic catalytic reactions in the CCS such as the lipase catalyzed esterification of oleic acid with 1-butanol and the synthesis of biodiesel from pure plant oils and methanol using a basic catalyst and the results will be reported in forthcoming papers. In addition, the data may also be valuable input for modeling of (reactive) extractions as well as for validation of CFD studies.

## Acknowledgements

Gerard Kwant, Iris Verschuren and Karla Danen of DSM are acknowledged for helpful discussions. John Janssen is acknowledged for assisting with the Lasentec® FBRM equipment. DSM and Schering-Plough are acknowledged for financial support through the Separation Technology program of the Netherlands Scientific Organization (NWO).

## References

[1] A. Stanckiewicz, J.A. Moulijn, Re-Engineering the Chemical Processing Plant: Process Intensification, Marcel Dekker, Inc., New York, 2004.
[2] G.J. Harmsen, Reactive distillation: the front-runner of industrial process intensification—a full review of commercial applications, research, scale-up, design and operation, Chem. Eng. Process. 46 (2007) 774–780.
[3] S. Kulprathipanja, Reactive Separation Process, Taylor & Francis, New York, 2002.
[4] H. Schmidt-Traub, A. Gorak, Integrated Reaction and Separation Operations, Springer, Berlin, 2006.
[5] J.C. Godfrey, M.J. Slater, Liquid–Liquid Extraction Equipment, John Wiley & Sons, New York, 1994.
[6] C. Hanson, Recent Advances in Liquid–Liquid Extraction, Pergamon Press Ltd., Oxford, 1971.
[7] J.D. Thornton, Science and Practice of Liquid–Liquid Extraction, Clarendon, Oxford, 1992.
[8] D.H. Meikrantz, L.L. Macaluso, H.W. Sams, C.H. Schardin, A.G. Federici, US Patent 5,762,800, 9 June 1998.
[9] G.J. Bernstein, D.E. Grosvenor, J.F. Lenc, N.M. Levitz, Annular centrifugal extractors, Nucl. Technol. 20 (1973) 200–202.
[10] N. Ruffer, U. Heidersdorf, I. Kretzers, G.A. Sprenger, L. Raeven, R. Takors, Fully integrated L-phenylalanine separation and concentration using reactive-extraction with liquid–liquid centrifuges in a fed-batch process with *E. coli*, Bioprocess Biosyst. Eng. 26 (2004) 239–248.
[11] J. Zhou, W.H. Duan, X.Z. Zhou, C.Q. Zhang, Application of annular centrifugal contactors in the extraction flowsheet for producing high purity yttrium, Hydrometallurgy 85 (2007) 154–162.
[12] X.Z. Zhou, J.Z. Zhou, C.Q. Zhang, W.D. Yu, Application of annular centrifugal contactor on separating indium from iron, Sep. Sci. Technol. 32 (1997) 2705–2713.
[13] J.Q. Zhu, J. Chen, C.Y. Li, W.Y. Fei, Centrifugal extraction for separation of ethylbenzene and octane using 1-butyl-3-methylimidazolium hexafluorophosphate ionic liquid as extractant, Sep. Purif. Technol. 56 (2007) 237–240.
[14] G.N. Kraai, F. van Zwol, B. Schuur, H.J. Heeres, J.G. de Vries, Two-phase (bio)catalytic reactions in a table-top centrifugal contact separator, Angew. Chem. Int. Ed. 47 (2008) 3905–3908.
[15] B. Schuur, J. Floure, A.J. Hallett, J.G.M. Winkelman, J.G. de Vries, H.J. Heeres, Continuous chiral separation of amino acid derivatives by enantioselective liquid–liquid extraction in centrifugal contactor separators, Org. Process Res. Dev. 12 (2008) 950–955.
[16] B. Schuur, A.J. Hallett, J.G.M. Winkelman, J.G. de Vries, H.J. Heeres, Scalable enantioseparation of amino acid derivatives using liquid–liquid extraction in a cascade of centrifugal contactor separators, Org. Process Res. Dev. 13 (2009) 911–914.
[17] B. Schuur, J.G.M. Winkelman, J.G. de Vries, H.J. Heeres, Experimental and modeling studies on the enantio-separation of 3,5-dinitrobenzoyl-(R), (S)-leucine by continuous liquid–liquid extraction in a cascade of centrifugal contactor separators, Chem. Eng. Sci. 65 (2010) 4682–4690.
[18] B. Schuur, B.J.V. Verkuijl, J. Bokhove, A.J. Minnaard, J.G. de Vries, H.J. Heeres, B.L. Feringa, Enantioselective liquid–liquid extraction of (R,S)-phenylglycinol using a bisnaphthyl phosphoric acid derivative as chiral extractant, Tetrahedron 67 (2011) 462–470.
[19] S. Vedantam, J.B. Joshi, Annular centrifugal contactors—a review, Chem. Eng. Res. Des. 84 (2006) 522–542.
[20] B. Schuur, W.J. Jansma, J.G.M. Winkelman, H.J. Heeres, Determination of the interfacial area of a continuous integrated mixer/separator (CINC) using a chemical reaction method, Chem. Eng. Process. 47 (2008) 1484–1491.
[21] K.E. Wardle, T.R. Allen, M.H. Anderson, R.E. Swaney, Analysis of the effect of mixing vane geometry on the flow in an annular centrifugal contactor, AIChE J. 55 (2009) 2244–2259.
[22] K.E. Wardle, T.R. Allen, M.H. Anderson, R.E. Swaney, Experimental study of the hydraulic operation of an annular centrifugal contactor with various mixing vane geometries, AIChE J. 56 (2010) 1960–1974.
[23] S.S. Deshmukh, S. Vedantam, J.B. Joshi, S.B. Koganti, Computational flow modeling and visualization in the annular region of annular centrifugal extractor, Ind. Eng. Chem. Res. 46 (2007) 8343–8354.
[24] S.S. Deshmukh, J.B. Joshi, S.B. Koganti, Flow visualization and three-dimensional CFD simulation of the annular region of an annular centrifugal extractor, Ind. Eng. Chem. Res. 47 (2008) 3677–3686.
[25] K.E. Wardle, T.R. Allen, R. Swaney, Computational fluid dynamics (CFD) study of the flow in an annular centrifugal contactor, Sep. Sci. Technol. 41 (2006) 2225–2244.
[26] K.E. Wardle, T.R. Allen, M.H. Anderson, R.E. Swaney, Free surface flow in the mixing zone of an annular centrifugal contactor, AIChE J. 54 (2008) 74–85.

[27] K.E. Wardle, T.R. Allen, R. Swaney, CFD simulation of the separation zone of an annular centrifugal contactor, Sep. Sci. Technol. 44 (2009) 517–542.
[28] K.R. Westerterp, W.P.M. van Swaaij, A.A.C.M. Beenackers, Chemical Reactor Design and Operation, Wiley, Chichester, 1987.
[29] E.E. Michaelides, Particles, Bubbles and Drops, World Scientific, New Jersey, 2006.
[30] J.C. Godfrey, in: J.C. Godfrey, M.J. Slater (Eds.), Liquid–Liquid Extraction Equipment, John Wiley & Sons, Chichester, 1994, pp. 363–409.
[31] G.A. Davies, in: J.D. Thornton (Ed.), Science and Practice of Liquid–Liquid Extraction, Clarendon Press, Oxford, 1992, pp. 244–342.
[32] H. Sawistowski, in: E. Alper (Ed.), Mass Transfer with Chemical Reaction in Multiphase Systems, Martinus Nijhoff Publishers, The Hague, 1983, pp. 613–635.
[33] J.C. Godfrey, C. Hanson, in: G. Hetsroni (Ed.), Handbook of Multiphase Systems, Hemisphere Publishing Corporation, Washington, 1982, pp. 4-1–4-46.
[34] L. Liu, O.K. Matar, E.S. Perez de Ortiz, G.F. Hewitt, Experimental investigation of phase inversion in a stirred vessel using LIF, Chem. Eng. Sci. 60 (2005) 85–94.
[35] D.R. Lide, CRC Handbook of Chemistry and Physics, 89th Ed., CRC Press, Cleveland, Ohio, 2008.
[36] D.M. Mitrinovic, A.M. Tikhonov, M. Li, Z.Q. Huang, M.L. Schlossman, Noncapillary-wave structure at the water–alkane interface, Phys. Rev. Lett. 85 (2000) 582–585.
[37] N.A. Terent'eva, G.I. Cherednichenko, Y. Nikulichev, Interfacial tension of some SF at the hydrocarbon–water interface, Chem. Technol. Fuels Oils 25 (1989) 404–406.
[38] A. Malzert, F. Boury, P. Saulnier, T. Ivanova, I. Panaiotov, J.P. Benoit, J.E. Proust, Interfacial properties of adsorbed films made of a PEG2000 and PLA50 mixture or a copolymer at the dichloromethane-water interface, J. Colloid Interface Sci. 259 (2003) 398–407.
[39] T. Sakka, K. Tanaka, Y. Shibata, Y.H. Ogata, Interfacial tension measurement at a flat liquid–liquid interface under electrochemical instability, J. Electroanal. Chem. 591 (2006) 168–174.
[40] R. Gunde, A. Kumar, S. Lehnert-Batar, R. Maeder, E.J. Windhab, Measurement of the surface and interfacial tension from maximum volume of a pendant drop, J. Colloid Interface Sci. 244 (2001) 113–122.
[41] B.A.A. van Woezik, K.R. Westerterp, Measurement of interfacial areas with the chemical method for a system with alternating dispersed phases, Chem. Eng. Process. 39 (2000) 299–314.
[42] M.D. Santiago, P. Trambouze, Perfectly agitated reactors with 2 liquid phases—measurement of interfacial area by chemical method, Chem. Eng. Sci. 26 (1971) 29–38.